Food Research International 192 (2024) 114680

Contents lists available at ScienceDirect

Food Research International

journal homepage: www.elsevier.com/locate/foodres

Structural and physical-chemical properties of milk fat globules fractionated by a series of silicon carbide membranes

Tobias Dons [a], Jacob J.K. Kirkensgaard [b], Victor Candelario [c], Ulf Andersen [d], Lilia Ahrné [a,*]

[a] Ingredient and Dairy Technology, Department of Food Science, University of Copenhagen, Rolighedsvej 30, DK-1958 Frederiksberg, Denmark
[b] Niels Bohr Institute, University of Copenhagen, Universitetsparken 5, 2100 Copenhagen, Denmark
[c] Departamento de Ingeniería y Ciencia de los Materiales y del Transporte, Escuela Politécnica Superior, Universidad de Sevilla, Calle Virgen de África 7, Seville 41011, Spain
[d] Arla Innovation Centre, Arla Foods amba., Agro Food Park 19, DK-8200 Aarhus-N, Denmark

ARTICLE INFO

Keywords:
Microfiltration
Milk fat globules
Milk fat separation
Small angle X-ray scattering
Confocal laser scanning microscopy
Silicon carbide membranes

ABSTRACT

Driven by the acknowledged health and functional properties of milk fat globules (MFGs), there is a growing interest to develop gentle methodologies for separation of fat from milk. In this study, separation of fat from raw milk and fractionation in streams containing MFGs of different size was achieved using a series of two silicon carbide ceramic membranes. A first step consisting of a 1.4 μm membrane aimed to concentrate the bulk of the fat, i.e. the larger MFGs (D[4,3] ~ 4 μm) followed by a 0.5 μm fractionation aimed to concentrate the residual milk fat in the permeate, i.e. fraction with the smaller MFGs (D[4,3] ~ 1.8–2.4 μm. The fat separation performance showed a yield of 92 % for the 1.4 μm membrane and 97 % for the 0.5 μm membrane. Both fat enriched retentates showed, by the confocal laser scanning microscopy, intact MFGs with limited damage in the MFG membrane. The fatty acid profile analysis and SAXS showed minor differences in fat acid composition and the crystallization behavior was related to differences in the fat content. The 0.5 μm permeate containing the smallest MFGs however showed larger aggregates and a trinomial particle size distribution, due to probably pore pressure induced coalescences. The series of silicon carbide membranes showed potential to concentrate some of MFGM proteins such as Periodic Schiff base 3/4 and cluster of differentiation 36 especially in the 0.5 μm retentates. A shift in casein to whey protein ratio from 80:20 (milk) to 50:50 was obtained in the final 0.5 μm permeate, which opens new opportunities for product development.

1. Introduction

During the last decade, the importance of commercial membrane filtration has increased radically in the dairy industry (France et al., 2021; Reig et al., 2021). The need for innovative applications, membrane materials and membrane functionality has become of crucial importance. The constant development of the dairies product portfolio will potentially increase the revenue resources in the dairy sector. Furthermore, the need to separate or concentrate health promoting compounds from milk has increased significantly. Membrane filtration proves as a suitable and economical alternative to many up-stream processes in the dairy industry such as bactofugation, centrifugation, standardization, demineralization and evaporation (Chenchaiah et al., 2013; Muthusamy, 2022).

Alternative processes for separation of native milk fat globules (MFGs) from milk has recently gained commercial interest, primarily due to their emulsifying properties in functional foods and the health benefits related to brain development in formula-fed babies (McCarthy et al., 2017). The MFGs range in the size from 0.1 to 15 μm and have a core consisting of triacylglycerols (Truong et al., 2020). A 5–50 nm trilayered membrane, termed the milk fat globule membrane (MFGM), consisting of phospholipids and glycolipids surrounds the triacylglycerols core. In raw milk, the MFGM keeps the MFG in a natural emulsion preventing physical degradation as coalescence, aggregation,

Abbreviations: Al_2O_3, Alumina; CSLM, Confocal light scanning microscopy; FA, Fatty Acid; LPL, Lipoprotein lipase; MFG, Milk Fat Globule; MFGM, Milk fat globule membrane; SAXS, Small-angle X-ray scattering; SDS-PAGE, Sodium dodecyl sulphate, polyacrylamide gel electrophoresis; SiC, Silicon Carbide; TiO_2, Titania; VCR, Volume concentration ratio; ZrO_2, Zirconia.

* Corresponding author.
E-mail address: lilia@food.ku.dk (L. Ahrné).

https://doi.org/10.1016/j.foodres.2024.114680
Received 8 May 2024; Received in revised form 17 June 2024; Accepted 26 June 2024
Available online 2 July 2024

enzymatic degradation by lipoprotein lipases and chemical degradation as oxidation (Lopez et al., 2010, 2011; Truong et al., 2020). The MFGM is embedded with membrane proteins, constituting 25–70 (% w/w) of the MFGM, such as Schiff base 3, 4, 6 and 7, xanthine oxidase, butyrophillin, and protease peptone 3 (Hansen et al., 2018; Muthusamy, 2022).These proteins are distributed integrally and peripherally in the membrane or loosely attached to the surface and have biological functions and health benefits (Hageman et al., 2019). It has previously been reported that the composition of small and large MFGs is considerably different due to differences in surface area and consequently differences in the content of milk fat globule membrane components which affect their functional properties (Lopez et al., 2011; Truong et al., 2016). Small MFGs have shown to have important health-promoting features in infant formula due to increased digestion rates affecting cognitive development in neonates (Chai et al., 2022).

Many processing steps in the dairy industry are known to affect the structure of the MFGM. Cooling shifts the MFGM affinity towards the serum phase, whereas heating causes complex formation between proteins and the exterior layer of the MFGM (Wiking et al., 2022). Upstream unit operations as transporting, agitation, pumping, centrifugation and pasteurization have previously been described to cause severe damage to the MFGM leading to membrane protein adsorption by whey proteins and caseins, which influences the functionality and health effects of milk (Holzmüller et al., 2016).

Jukkola et al. (2019), Hansen et al. (2019), and Dons et al. (2023, 2024) demonstrated the potential of ceramic membranes to separate milk fat and keep intact MFGs. Michalski et al. (2006) fractionated MFGs into smaller (D[4,3] 0.9–3.3 μm) and larger (5.0–7.5 μm) fat globules using Al_3O_2 membranes with pore sizes ranging from 2 μm pore size with up to 95 % fat recovery to 12 μm pore size with 12 % fat recovery.

Silicon carbide (SiC) ceramic membranes with pore sizes of 0.5 and 1.4 μm have previously shown superior performance in regards to yield, fat concentration and MFG intactness (Dons et al., 2023, 2024). Although, the use of membranes in series have the potential to enable gentle fractionation of smaller and larger MFGs, to the best of our knowledge such process has not yet been reported.

Thus, the objective of this study is to generate new insights on (i) the fractionation of MFGs from raw milk by size using a series of hydrophilic SiC ceramic membranes and (ii) the properties of the streams obtained. The sequential filtration of raw milk using the SiC membranes of varying pore size (1.4 and 0.5 μm) is expected to improve the fractionation efficiency compared to a single-stage filtration and produce streams with unique characteristics in terms MFG sizes and casein to whey protein ratio. The 1.4 μm filtration is expected to produce a retentate containing MFGs with a wider range of sizes, while the 0.5 μm membrane is expected to narrow the size range and concentrate the smaller milk fat globules. The membrane filtration performance will be investigated in terms of flux behavior, and the properties of the streams will be analyzed in terms of particle sizes, surface charges. Further, fatty acid profile and scattering techniques as small angle x-ray scattering (SAXS) will be used to characterize the fat fractions.

2. Materials and methods

2.1. Membranes and milk

Liqtech Ceramics A/S (Ballerup, Denmark) supplied two SiC tubular ceramic membranes for microfiltration with a surface area of 0.333 m^2 and the dimensions: length of 1178 mm, an outer diameter of 25 mm, a channel width of 3 mm and 30 channels. The pore size of the SiC membranes were 0.5 and 1.4 μm.

The bovine raw milk used, was collected during summer from a local Danish organic farm (Mannerup Møllegaard, Osted, Denmark) from grazing Danish red cows and stored at 4 °C until processed further. Composition of the raw milk was determined by MilkoScan FT2 (Foss Analytics, Hillerød, Denmark) and may be observed in Table 1. The composition of the raw milk, now considered as the feed of the filtration process contained on average 4.5 % fat, 3.5 % protein where 2.5 % consisted of casein, and the amount of total solids were 13.5 %. All chemicals were of analytical grade and used according to Dons et al. (2023; 2024). All samples were measured using the MilkoScan FT2 at different calibrations depending on fat content due the fast and accurate measures.

2.2. Pore size distribution of membranes

The pore size distribution of the 0.5 and 1.4 μm membranes were analyzed by capillary flow porometry previously described by Dons et al. (2023). The pore pressure range for the 1.4 μm membrane was 0.6–2.0 μm, while for the 0.5 μm membrane the pore pressure range was 0.2–4.0 μm due to the smaller pores.

2.3. Membrane processing and filtration performance

The filtration trials were carried out in triplicate in batch using a commercial SW25 pilot scale membrane system from MMS Nordic (Urdorf, Switzerland) as previously described by Dons et al. (2023, 2024).

The clean water permeability of the membranes was initially determined at 45–50 °C using regular tap water assessed according to Dons et al. (2023; 2024), and the values measured to 2963 $L{\cdot}h^{-1}{\cdot}m^{-2}{\cdot}bar^{-1}$ for the 1.4 μm and 2579 $L{\cdot}h^{-1}{\cdot}m^{-2}{\cdot}bar^{-1}$ for the 0.5 μm membrane. Both membranes were fully cleanable with a permeability recovery ratio >0.90. The crossflow velocity of the milk fat separation process was stable at ≈6.0 $m{\cdot}s^{-1}$, whereas for the water permeability it was stable at ≈6.6 $m{\cdot}s^{-1}$ with a ΔP of 0.44–47 bar.

A Microthermics UHT/HTSL lab-25 EHVH (Raleigh, NC, USA) continuous flow heater was used to heat 24 L of raw milk to 53 ± 2 °C and added to the preheated feed tank (50 °C). The raw milk was separated at ≈50 °C on the SW25 mounted with the 1.4 μm SiC membrane at 0.30 bar transmembrane pressure. The separation was performed until a volume concentration ratio (VCR) 4 was reached. During the separation 18 L of permeate was collected in an ice cooled bucket to reach 7 °C rapidly, and at the end of the filtration stored at 4 °C. After the filtration,

Table 1
The abundant measurements of the different membranes used. Values are presented as mean ± standard deviation; superscripts $^{a-f}$ ($P \leq 0.05$) denotes significant difference between pore size and VCR.

Membrane pore size [μm]	Sample	Fat [% w/w]	Total solids[% w/w]	Protein [% w/w]	Casein [% w/w]	Particle Size D[4,3] [μm]
1.4	Feed	4.48 ± 0.22^{a}	13.49 ± 0.24^{a}	3.45 ± 0.06^{a}	2.53 ± 0.00^{a}	4.13 ± 0.12^{a}
	VCR 2	8.27 ± 0.22^{b}	16.67 ± 0.30^{b}	3.38 ± 0.02^{a}	2.40 ± 0.15^{a}	4.32 ± 0.08^{a}
	VCR 3	11.64 ± 0.21^{c}	19.77 ± 0.23^{c}	3.17 ± 0.00^{b}	2.38 ± 0.03^{b}	4.35 ± 0.09^{a}
	VCR 4	16.34 ± 0.37^{d}	24.10 ± 0.27^{d}	3.16 ± 0.09^{b}	2.30 ± 0.04^{b}	4.41 ± 0.11^{b}
0.5	Permeate/Feed	0.51 ± 0.03^{e}	9.67 ± 1.14^{e}	3.43 ± 0.05^{a}	2.75 ± 0.05^{c}	1.82 ± 0.14^{c}
	VCR 2	1.56 ± 0.12^{f}	11.13 ± 1.51^{a}	4.64 ± 0.23^{c}	3.26 ± 0.04^{d}	2.29 ± 0.16^{c}
	VCR 3	2.39 ± 0.56^{g}	12.36 ± 1.35^{a}	6.06 ± 0.41^{d}	4.54 ± 0.61^{e}	2.41 ± 0.11^{e}
	Permeate	0.19 ± 0.05^{e}	8.53 ± 0.08^{e}	4.05 ± 0.07^{e}	2.11 ± 0.02^{f}	9.20 ± 1.12^{f}

5.5–6.0 L of retentate was collected and cooled to 4 °C and stored. The 1.4 μm membrane was then cleaned according to Dons et al (2023). After cleaning the SiC 1.4 μm membrane was dismounted from the SW25 and mounted with the 0.5 μm membrane, the water permeability was checked and the feed tank heated to ≈50 °C. The 18 L of collected permeate from the SiC 1.4 μm separation was then heated using the Microthermics to 53 ± 2 °C and added to the preheated feed tank. Separation of the SiC 1.4 μm permeate was then performed until VCR 3 resulting in 12 L of permeate and 6 L of retentate. The SiC 0.5 μm was then cleaned and dismounted from the SW25. All streams from the SiC 1.4 and 0.5 μm were stored at 4 °C until further analysis the following day. The yield was determined was determined as the amount of fat recovered from the feed according to Dons et al. (2023, 2024).

2.4. Physiochemical analysis of streams

2.4.1. Total protein content and casein content of streams

The total nitrogen content of feed, retentate and permeate was measured by Dumas using an Nrapid Max exceed (Elementar, Langenselbold, Germany). Initially, 250 ± 1 mg of aspartic acid was added to the combustion containers for standardization, followed by addition of 2 mL of each sample in combustion containers and the exact weight was noted. A conversion factor of 6.38 was used to convert total nitrogen to protein content (Maubois and Lorient, 2016).

Casein content was measured by adding 0.1 M urea to the samples and centrifuged at 30.000× *g* for 10 min. The supernatant was then collected, and washed two times with similar conditions. Supernatant was then measured by Dumas in combustion containers and subtracted from the total protein content.

2.4.2. Particle size distribution of MFGs in the streams

The particle size distribution of feed, retentate and permeate of the SiC 1.4 and 0.5 μm membranes was measured by static light scattering using a Mastersizer 3000 (Malvern Instruments, Malvern, UK). The refractive index of the samples was set at 1458 (real part) and 0.001 (imaginary part). The sample was added into MiliQ water (refractive index 1.33) as dispersion medium, to an obscuration ≈6 % and particle size distribution was immediately recorded, three readings were conducted for each sample. The D[4,3] – De Brouckere Mean Diameter was obtained from the Mastersizer 3000 software v3.62.

2.4.3. Zeta potential indicating mechanical damage of treated MFGs

The MFGs in the mentioned samples were measured by dynamic light scattering using a Zetasizer NANO ZS90 (Malvern Instruments, Malvern, UK) and parameters set according to Michalski et al., 2001. Samples were diluted 100 fold in simulated milk ultra-filtrate and measured in a Malvern capillary cell DTS 1070 (Malvern Instruments, Malvern, UK) at 20 °C with an initial equilibrium time of 2 min and three readings of each sample.

2.4.4. Structure and integrity of MFG and MFGM

The microstructure and integrity of the MFG and MFGM was observed using an inverted SP5 microscope (Leica Microsystems GmbH, Wetzlar, Germany) confocal laser scanning microscopy (CLSM) mounted with a Helium/Neon laser and a 63× (1.4 numerical aperture) magnification oil immersion objective was used with a resolution of 1024 × 1024 pixels to capture images. The Helium-Neon laser operated at an excitation wavelength of 543 nm and emission wavelength from 565 to 615 nm to detect the fluorescent molecules adapted from Lopez et al. (2011).

2.4.5. MFGM profiling of proteins in generated streams

Feed, retentate and permeate samples from the 1.4 and 0.5 μm separation processes was measured for MFGM associated proteins by sodium dodecyl sulfate–polyacrylamide gel electrophoresis (SDS-PAGE). After an initial washing of fat the samples were dispersed in (1:3 w/w) 50 mM Tris-HCL buffer, containing 10 % glycerol and 5 % sodium dodecyl sulphate (SDS) at pH 6.8, followed by SDS-PAGE where analysis of the proteins from the samples was done under non-reduced and reduced conditions using 1 M dithiothreitol (DTT Invitrogen, Naerum, Denmark) for 20 min at 40 °C. Reduced and non-reduced samples were added to NuPAGE Novex 4–12 % Bis-tris gels (Invitrogen, Naerum, Denmark) with the loading of 5 μL of each prepared sample. 3 μL milk proteins broad-range SDS-PAGE molecular mass standards (BIO-RAD, Hercules, Ca, USA) were loaded to the gels and the electrophoretic separation was performed by applying a voltage of 200 V for 50–55 min. After the staining with 1 % Coomassie Blue and destaining of the gels with 10 % acetic acid. Images were captured using an Epson Perfection V750 pro Scanner (Epson, Nagano, Japan) with the following image software (TotalLab100; Nonlinear, Dynamics, Durham, NC, USA). The MFGM associated proteins were identified by the molecular weight of the protein band markers and previous studies (Hansen et al., 2019, 2020; Jukkola et al., 2019; Yang et al., 2021).

2.4.6. Small-angle X-ray scattering (SAXS) of MFGM interactions

Feed, retentate and permeate samples for the 1.4 and 0.5 μm membranes were measured by SAXS using a Nano-inXider instrument from Xenocs SAS (Grenoble, France) having a 40 W micro focused copper source (Rigaku-Denki, Co., Tokyo, Japan) producing X-rays with a wavelength of λ = 0.154 nm. The Nano-InXider was mounted with a Pilatus 100 k pixel-detector from Dectris (Baden, Switzerland) measuring the scattering in a q-range from 0.001 to 0.4 $Å^{-1}$ where the scattering vector is given by theta being the scattering angle:

$$q = \frac{4\pi}{\lambda} sin(\theta) \quad (1)$$

The 2D detector images were azimuthally averaged to produce the 1D intensity (I) curves as a function of q for the different samples. All samples were measured in borosilicate capillary tubes with an inner diameter of 1.48 mm sealed with wax and paraffin glue. The permeate and retentate samples were background subtracted with MiliQ water. All samples were measured at high resolution for 60 min at firstly 7 °C and then at 50 °C to simulate either storage or processing conditions. All background subtraction and data reduction were performed using the XSACT software package.

2.4.7. Fatty acid profiles of the streams

The fatty acids (FA) of the milk fat in raw milk, retentate and permeate samples were extracted, and derivatized (methylated), and analyzed by gas chromatography flame ionization detection (GC-FID). Each sample (≈30 mg) was extracted with 1.5 mL of dichloromethane: methanol solution (8:2 *v*/v) in a Mixer Mill MM40 (Retsch Technology, Haan, Germany). The sample tubes were then centrifuged for 8 min at 10,000× *g* and 4 °C. After the centrifugation, the dichlormethane phase was collected and the precipitate was washed with dichloromethane: methanol solvent 3 times in total along with repeating centrifugation (7,000× *g*, 10 min). The dichloromethane phase in the samples was evaporated by nitrogen injection to dryness. The fat extracts containing at least 10 mg fat were added 1.0 mL of sodium methylate and incubated at 65 °C in a water bath for 40 min. 4 mL of saturated sodium chloride and 1.0 mL of hexane were then added to the solutions and mixed thoroughly.

After separation, the hexane phase was collected and evaporated once unnder nitrogen and re-dissolved in 0.5 mL hexane. The samples were then injected into the GC with 1 μL (HP 6890 Series mounted with an FID, Agilent Technologies, Santa Clara, USA) with 1:25 split-flow and analyzed at constant flowrate of 1 $mL{\cdot}min^{-1}$. The injection temperature was set to 250 °C and the temperature of detection to 300 °C. The methylated FAs were separated on an Omegawax TM 320 fused-silica capillary column (30 m × 0.32 mm × 0.25 μm film thickness), with hydrogen as carrier gas and the following oven temperature program:

50 °C for 1 min, then increased by 15 °C·min^{-1}–180 °C followed by 3 °C·min^{-1}–240 °C kept constant for 10 min. The FAs were identified by comparison with alkane standard (C4–C24). The effects of processing were on the level of FAs estimated based on the peak areas. The method was modified and adapted from Buldo, et al. (2013) and (Yang et al., 2021).

2.5. Statistical analysis

Means were analyzed by one-way and two-way analysis of variance (ANOVA) followed by Tukey multiple comparison test for statistical significance $P \leq 0.05$ in the software R-Studio (version, 2023.03.0+386). All physical and chemical analysis were conducted in triplicates for each of the three filtration trials.

3. Results and discussion

3.1. Evaluation of serial membrane performance and yield

The permeate flux for the two membranes at 50 °C is shown in Fig. 1, where a clear difference in the filtration performance is observed. Both filtrations were conducted at a transmembrane pressure of 0.30 bar. The filtration performance shows, that the 1.4 μm membrane took 18 min to reach a VCR of 4. During this period a heavy flux decline of 51 % occurred from 204 to 99 L·h^{-1}·m^{-2}, while concentrating the fat from 4.48 ± 0.22 % to 16.34 ± 0.37 % (See Table 1). The major flux decline is mainly due to formation of the concentration polarization layer on top of the membrane that is widely recognized to consist of both proteins and fat and cause pore shrinkage, pore blocking and consequently fouling. Similar work conducted by Hansen et al. (2020) (TiO_2, 0.8 and 1.4 μm), Jukkola et al. (2016, 2019), (Al_2O_3, 1.4 μm) and Dons et al. (2023, 2024), (SiC, 1.4 and 0.5 μm) showed similar flux decline during the filtration. Though, Jukkola el al., (2019) and Hansen et al. (2020) utilized diafiltration to decrease the fouling reducing in this way the permeate flux decline.

The collected permeate after the 1.4 μm membrane filtration with a fat content of 0.51 ± 0.03 % (see Table 1) was concentrated to VCR 3 with 0.5 μm membrane during 69 min with a 40 % flux decline from 39 to 24 L·h^{-1}·m^{-2}. Results reported by Dons et al. (2024) using raw milk showed significantly longer processing times (121 versus 69 min). This might indicate that the larger MFGs in milk reduce the permeate flux, when using membranes with such a small pore size. Hypothetically, the MFGs will hinder the permeate flux by blocking the membrane pores due to their size, when the concentration of fat increases with increasing VCR. The final fat content of the 0.5 μm VCR 3 retentate was 2.39 ± 0.56 % fat, while the permeate contained 0.19 ± 0.05 % fat.

The yield of the filtration process was determined as the amount of fat recovered from the feed stream to the retentate. In this case, the raw milk is the feed for the 1.4 μm filtration process and the permeate obtained form 1.4 μm filtration is the feed for the 0.5 μm filtration process. At VCR 4 the 1.4 μm membrane retained up to 92.3 ± 1.4 % of the fat, while the 0.5 μm membrane reached a maximum VCR of 3 with 97.0 ± 0.2 % fat retention. At VCR 2 there was an insignificant yield difference between the two membranes (1.4 μm = 92.3 ± 2.3 % and 0.5 μm = 95 ± 0.7 %). The 0.5 μm membrane had a significantly higher yield at VCR 3 (97 ± 0.23 %), compared to the 1.4 μm membrane. Dons et al. (2024) showed up to 90, 97 and 91 % fat retention using SiC 1.4 μm, 0.5 μm and ZrO_2 on SiC support 0.06 μm membranes respectively. Hansen et al. (2020) showed up to 97 % fat retention using TiO_2 0.8 and 1.4 μm membranes and diafiltration, while Jukkola et al. (2019) showed up 93 % fat retention with an Al_2O_3 1.4 μm membrane.

3.2. Psychochemical properties of the fractions

3.2.1. Particle size distribution

The particle size distribution of MFGs in the feed, permeate and retentate stream for the two membranes at VCR 2–4 are shown in Fig. 2, and the volume mean diameter D[4,3] are shown in Table 1.

Fig. 2A shows the 1.4 μm retentates, similarly to the raw milk (feed), consist to large extent of MFGs with size ranging from 1 to 10 μm. An

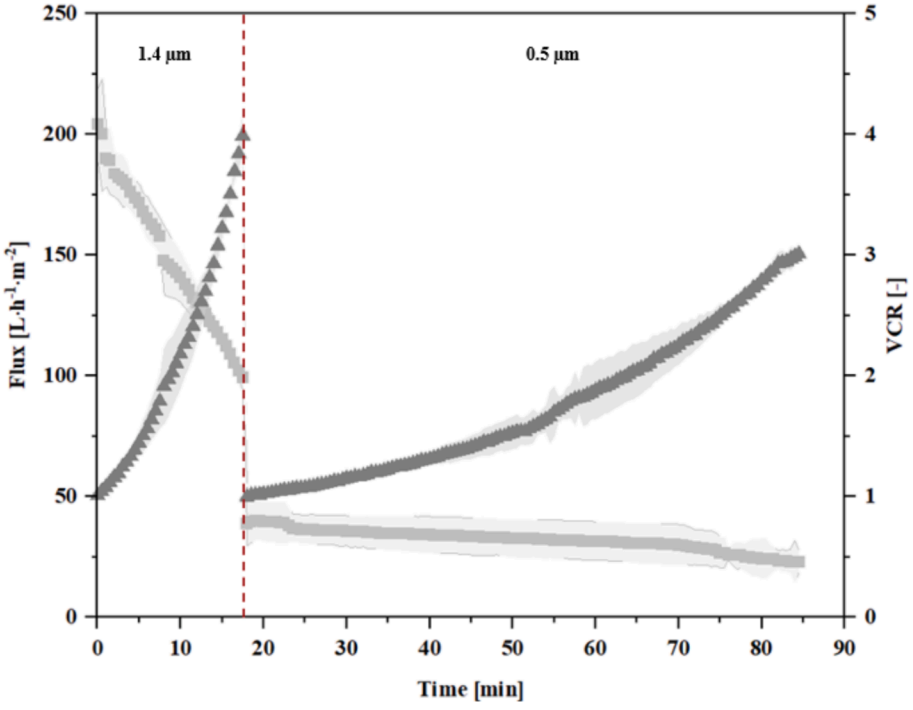

Fig. 1. ■ The permeate flux of the process at constant transmembrane pressure of 0.30 bar for the two different membranes in series as a function of time. ▲ The increasing VCR for the two membranes, where the 1.4 μm membrane reached a VCR of 4, and the 0.5 μm membrane reached a VCR of 3.

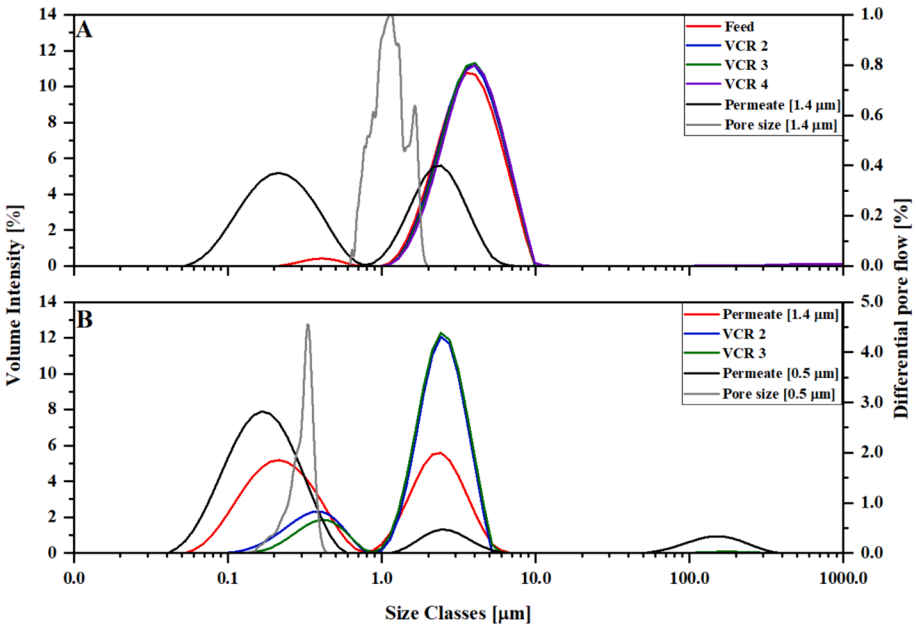

Fig. 2. (A) The 1.4 µm membrane pore size distribution, with the particle size distribution of raw milk as feed, the 1.4 µm permeate and 1.4 µm retentate from VCR 2–4. (B) The 0.5 µm membrane pore size distribution, with the particle size distribution of 1.4 µm permeate as feed, the 0.5 µm permeate and 0.5 µm retentate from VCR 2–3.

increase in volume intensity from feed to the final VCR of 4 is observed and the D[4,3] also show a statistically significant increase from 4.13 ± 0.12 µm for the feed to 4.35 ± 0.09 µm at VCR 4 (Table 1). The increase in D[4,3] is primarily due to the permeation of small fat globules into the permeate stream. As shown in Fig. 2A the 1.4 µm permeate stream has a clear permeation of fat globules (<0.8 µm) smaller than the pore size, but also a significant volumes of fat globules larger than the 1.4 µm pore size were able to permeate through the membrane, resulting in a volume mean diameter of 1.82 ± 0.14 µm.

Fig. 2B shows the 0.5 µm filtration using the 1.4 µm permeate as feed. The retentates, similar to the permeate/feed of 1.4 µm filtration, show a bimodal particle size distribution with a population ranging from ≈0.03–0.8 µm and another from ≈1–5 µm. However, the retentates show a significant increase in the volume intensity of the population with large MFGs and decrease of the smaller MFGs compared with the feed, consequently the D[4,3] significantly increased from 1.82 ± 0.14 µm to 2.41 ± 0.12 µm at VCR 3.

Permeation of the small fat globules (<0.4 µm) was observed in the 0.5 µm permeate, which also contained a small volume of large MFGs (1–4 µm) and large aggregates at (50–200) µm resulting in a trinomial distribution. Thus, the D[4,3] of this stream was 9.20 ± 1.12 µm. The large aggregates may have been formed from coalescence of damaged MFGs, which pass freely through the 0.5 µm membrane, as the filtration was carried out at 50 °C, i.e. above the melting range of milk fat (−40 to 40 °C) (Dewettinck et al., 2008). The damaged fat globule could hypothetically be squeezed through the membrane pores, which may cause pressure induced coalescence consequently forming large milk fat globules with either shared MFGM material or coverage with serum proteins. Previous studies by Michalski et al. (2002) observed similar tendencies for comparison of native vs damaged fat globules. Further, Yang et al. (2021) reported similar results where a small peak of aggregates (≈180 µm) was observed for heavy processed milk using pulsed electric fields. This may indicate that extended pumping or interactions in the membrane pore flow affects the emulsion stability of the MFGs in the final permeate.

3.2.2. Composition of retentates and permeates

The composition of the feed permeate and retentate streams for both membrane filtrations including fat, protein, total solids and relative casein content is shown in Table 1. As expected, the experimental outcome for the composition showed a proportional increase in fat content in retentates with increasing VCR.

In the first filtration step, using the 1.4 µm membrane, the retentate stream reached ≈16 % of fat at VCR 4 containing large MFGs. The second step, used the 0.5 µm membrane to concentrate the 1.4 µm permeate, achieving a retentate with ≈2 % fat at VCR 3 containing smaller MFGs. The initial filtration of raw milk using the 1.4 µm showed a 44 % increase in total solids from 13.49 ± 0.24 % to 24.10 ± 0.27 % (w/w) due to the increase in fat content. However, the protein content decreased from 3.45 ± 0.06 to 3.16 ± 0.09 % w/w due to loss of milk proteins through the membrane. This is consequently observed in the permeate containing ≈0.5 % fat, while containing ≈10 % total solids with 3.43 ± 0.05 % protein. The further concentration of this permeate stream with the 0.5 µm membrane resulted in an increase of fat content from ≈0.5 to 2.39 ± 0.56 %. Further, the SiC membrane was also able to concentrate the protein content from 3.43 ± 0.05 to 6.06 ± 0.41 %. The relative casein content showed that the 0.5 µm membrane concentrated the caseins in the 0.5 µm retentate. The 0.5 µm permeate primarily consisted of whey proteins resulting in a whey-like stream with high protein content.

Analyzing now the data, as % per total solids, a clear difference of fat and protein per total solids can be observed in Fig. 3. Fig. 3A shows in the retentate a significant increase in % fat per total solids, while showing a significant decrease in protein per total solids from VCR 2 to VCR 4. The decrease in protein content is primarily due to the open pore structure of the 1.4 µm membrane, which allows clear permeation of both caseins (0.04–0.3 µm), whey proteins (13–19 kDa) and potentially whey protein aggregates (0.01–0.1 µm) (Purwanti et al., 2011).

Most importantly a clear increase > 50 % on %fat per total solids is observed comparing Fig. 3C (feed) and Fig. 3A (retentate) at VCR 4. Similar increase is seen in Fig. 3D and 3B µm for the 0.5 µm membrane.

The 0.5 µm membrane concentrated 23 % of the % protein per total solids during the filtration to VCR 3. The final protein concentration of the Fig. 3E VCR 3 stream was 61 $g{\cdot}L^{-1}$. Previously Qi et al. (2022) used a 0.1 µm α-Al_3O_2 to concentrate protein in skimmed milk to VCR 2 resulting in a total protein content of 45 $g{\cdot}L^{-1}$. Even though the SiC 0.5 µm membrane has a larger pore size, it was still able to achieve a higher final protein content, potentially due to considerable higher

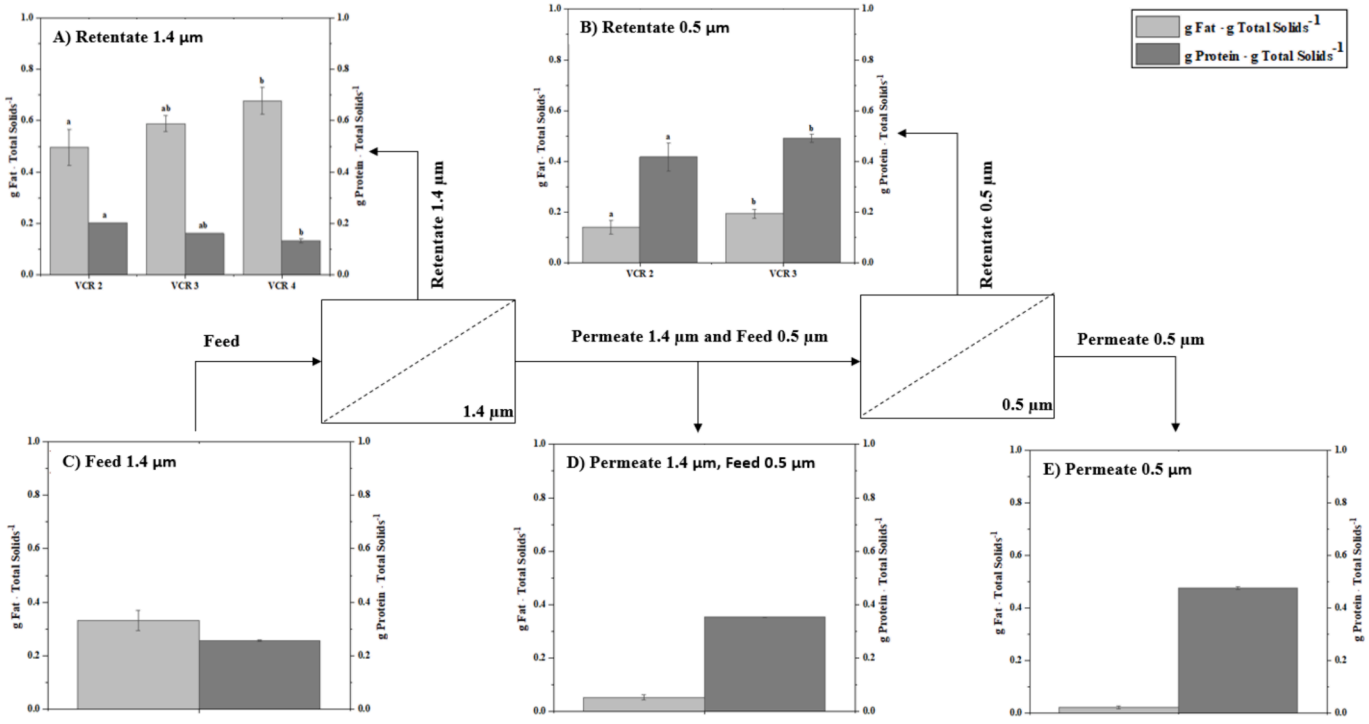

Fig. 3. (A) Content of fat and protein per total solids for the retentate VCR 2–4 streams, (B) the 0.5 µm retentate at VCR 2 and 3, (C) the Feed for the 1.4 µm filtration (D) the 1.4 µm permeate used for the 0.5 µm filtration and (E) the 0.5 µm permeate. The results are presented as mean ± standard deviation superscripts [a–b] denotes significant differences in graphs ($P \leq 0.05$).

hydrophilicity and lower zeta potential of the SiC material (≈−30 mV, pH 6.8) compared to α-Al_3O_2 (Dons et al., 2024). This might indicate that membrane surface properties has a higher impact on membrane filtration processes than previously assumed.

The filtration of the 1.4 µm permeate resulted in a shift in casein to whey protein ratio 80:20 in the initial raw milk, to ≈50:50 in the final 0.5 µm permeate (Fig. 3E). Both permeate streams attributed valuable compositional features, which could be highly applicable in the production of low fat cheeses as previously described by Xia et al. (2020).

3.2.3. *Fatty acid profile and fat crystallization*

The results from fatty acid profile (FA) obtained by GC-FID analysis is shown in Table 2. The retentates from 1.4 and 0.5 µm filtration at maximum VCR (4 and 3 respectively) showed a significant higher content of short chain fatty acids > 8.5 % (C4:0–C10:0) compared to the initial feed. Further, these streams also contained a higher total amount of saturated FA. However, no significant differences are observed between the retentates of the 1.4 µm filtration (with D[4,3] = 4.41 ± 0.11 µm) and the retentates of the 0.5 µm filtration (with D[4,3] 2.23 ± 0.11 µm). Clear similarities were also found between the FA profiles of the feed and the 1.4 µm permeate, even here the average sizes of the MFGs were different (Feed D[4,3] = 4.1 µm and 1.4 µm permeate D[4,3] = 1.82 ± 0.14 µm). The two streams contained similar amounts of saturated fatty acids from C12:0–C16:0 and insignificant amounts of short chain fatty acids C4:0–C10:0, stearic acid (C18:0), oleic acid (18:1) and linoleic acid (18:2). The increased amount of short chain FAs in VCR 4, VCR 3 and 0.5 µm permeate samples may originate from breakdown of the longer chained FA e.g. C14:0, C16:0 and C18:0. The long chained

Table 2
Fatty acid composition (g·100 g^{-1} of FA) in the feed, maximum retentate and permeate samples treated with the 1.4 and 0.5 µm filtration. Results are presented as mean ± standard deviation. The different lower case letters (a–d) in the same row indicates significant differences ($P \leq 0.05$). The sum is accumulated to less than 100 %, since minor peaks not identified were left out from the table.

Fatty acid [%]	Feed	1.4 µm VCR 4	0.5 µm VCR 3	1.4 µm permeate	0.5 µm permeate
C4:0	0.53 ± 0.40^{b}	2.31 ± 0.23^{a}	2.16 ± 0.03^{a}	0.20 ± 0.14^{b}	2.00 ± 0.24^{a}
C6:0	1.34 ± 0.59^{ac}	2.22 ± 0.17^{b}	2.18 ± 0.02^{b}	0.87 ± 0.14^{c}	2.08 ± 0.01^{ab}
C8:0	1.18 ± 0.19^{bc}	1.42 ± 0.01^{ac}	1.45 ± 0.03^{a}	1.05 ± 0.05^{b}	1.43 ± 0.02^{a}
C10:0	3.24 ± 0.09^{b}	3.38 ± 0.03^{a}	3.39 ± 0.01^{a}	3.21 ± 0.03^{b}	3.32 ± 0.06^{ab}
C12:0	4.07 ± 0.02^{a}	4.07 ± 0.01^{a}	4.07 ± 0.01^{a}	4.21 ± 0.03^{b}	4.06 ± 0.11^{a}
C14:0	13.10 ± 0.03^{a}	12.78 ± 0.05^{a}	12.74 ± 0.01^{a}	13.40 ± 0.12^{b}	12.68 ± 0.11^{a}
C14:1	1.15 ± 0.03^{ab}	1.08 ± 0.01^{b}	1.12 ± 0.04^{b}	1.17 ± 0.02^{a}	1.16 ± 0.01^{ab}
C15:0	1.27 ± 0.06^{bc}	1.19 ± 0.04^{ab}	1.16 ± 0.00^{ab}	1.22 ± 0.00^{c}	1.21 ± 0.04^{a}
C16:0	35.20 ± 0.51^{ab}	33.61 ± 0.26^{c}	34.00 ± 0.08^{ac}	35.53 ± 0.10^{b}	34.52 ± 0.31^{ab}
C16:1	1.58 ± 0.04^{b}	1.52 ± 0.01^{ac}	1.47 ± 0.05^{a}	1.60 ± 0.02^{bc}	1.57 ± 0.04^{ab}
C17:0	0.63 ± 0.02^{a}	0.60 ± 0.02^{a}	0.58 ± 0.02^{a}	0.60 ± 0.03^{a}	0.60 ± 0.01^{a}
C18:0	12.18 ± 0.82^{a}	11.97 ± 0.43^{ab}	11.54 ± 0.11^{bc}	12.02 ± 0.10^{a}	11.38 ± 0.14^{b}
C18:1 c(n9)	19.13 ± 0.46^{bd}	18.70 ± 0.05^{c}	19.19 ± 0.07^{ac}	19.74 ± 0.15^{d}	18.94 ± 0.15^{ab}
C18:2 t(n6)	2.34 ± 0.03^{a}	2.20 ± 0.05^{ab}	2.20 ± 0.05^{b}	2.33 ± 0.01^{a}	2.23 ± 0.10^{a}
C18:3 (n3)	1.25 ± 0.16^{b}	1.22 ± 0.13^{ab}	1.18 ± 0.02^{a}	1.12 ± 0.01^{ab}	1.12 ± 0.02^{ab}
C20:0	0.25 ± 0.01^{a}	0.24 ± 0.03^{a}	0.22 ± 0.00^{a}	0.23 ± 0.02^{a}	0.23 ± 0.02^{a}
C20:1 (n9)	0.48 ± 0.01^{a}	0.51 ± 0.03^{a}	0.39 ± 0.02^{a}	0.52 ± 0.03^{a}	0.56 ± 0.06^{a}

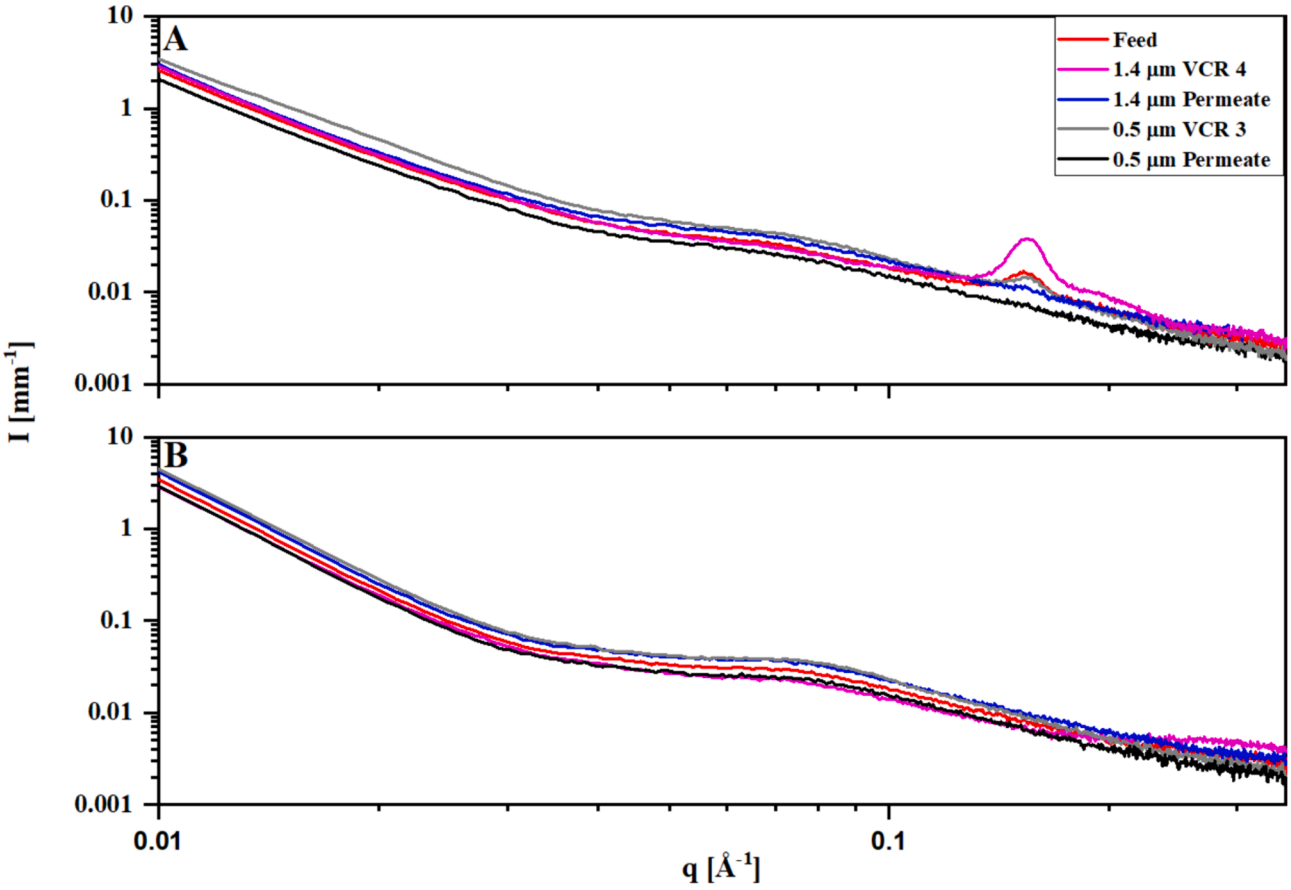

Fig. 4. SAXS data for the generated samples at (A) storage temperature 7 °C and (B) processing temperature 50 °C. The q-region of interest was set from 0.01 to 0.35 $Å^{-1}$ for fat crystallization and casein structure.

fatty acids may be labile due to the several heating and cooling steps and extended pumping (Michalski et al., 2006). The short chain FAs are generally known to cause rancid flavors in milk and milk products due to e.g. indigenous lipases as lipoprotein lipases (LPL) that cause spontaneous lipolysis of the long chained fatty acids (Deeth, 2006, 2011). In the case of the 0.5 µm permeate, this might be due to the association of LPL to the casein micelle, which are permeating through the membrane (Dickow et al., 2011). This would cause an increased content of LPL in the 0.5 µm permeate containing some large MFG aggregates (9.2 µm) with limited integrity, making the MFG core easy accessible for lipases.

Briard et al. (2003) and Lopez et al. (2011) both used microfiltration to separate MFGs into different size classes, observing differences in FA profile between feed and retentates. Briard et al. (2003) reported small MFGs ranging from D[4,3] = 1.50–3.26 µm and large globules from D[4,3] = 5.92–7.34 µm, while Lopez et al. (2011) reported D[4,3] = 1.6 ± 0.2 µm for small MFGs and for the large MFGs a D[4,3] = 6.5 ± 0.1 µm. They both reported a higher content of unsaturated FAs in streams containing small fat globules and an increased amount of long chain FAs in the large MFGs. This was though not observed in this study, due to smaller MFG sizes in the milk compared to the ones previously reported. It is hard to compare studies conducted with milk from different origin, animal feeding and seasons due to raw milk variations affecting the size distribution (Thum et al., 2023).

SAXS was used to investigate the crystallization of milk fat in the generated streams. Fig. 4 shows the Small-angle X-ray scattering (SAXS) data of the streams obtained at maximum VCR assessed at 7 °C, where crystallization peaks are expected to be observed, and at 50 °C which was the filtration temperature. In the high q-range 0.1–0.2 Å-1 a clear peak is observed for the samples containing fat (Feed (≈4.5 % fat), 1.4 µm retentate (≈16.4 % fat) and 0.5 µm retentate (≈2.4 % fat)). As expected the 0.5 µm VCR 3 peak had a small intensity decrease compared to the feed due to the lower fat content, while a large peak is observed for the 1.4 µm VCR 4. The low fat samples as the 1.4 µm permeate and 0.5 µm permeate showed no peak in this region. In addition to the differences in concentration no other difference were observed by SAXS in the samples. Previous studies by both Buldo et al. (2013) and Kaufmann et al. (2013) investigated different milk fats by SAXS, describing the peak between 0.1 and 0.2 Å-1 as crystallization of the triglycerides inside the MFGs. This peak is not present in Fig. 4B, where the samples are measured at 50 °C, indicating that the crystal structure in the triglyceride core of the MFGs is liquid during processing.

3.3. Structure of MFG and MFGM

3.3.1. Milk fat globule morphology

Confocal laser scanning microscopy was assessed to determine the overall integrity of the MFGs and the MFGM in both retentate (Fig. 5) and permeate (Fig. 6) samples. Staining of the samples were done for the carbohydrate moieties of the glycoproteins (red) and membrane phospholipids (yellow) present in the MFGM.

The raw milk used as feed and the final retentates (VCR 4) for the 1.4 µm and 0.5 µm filtrations are shown in Fig. 5. All samples from the CLSM micrographs in both feed and retentate showed intact MFGMs with almost entirely covered MFGs with phospholipids and glycoproteins. The serum ordered black domains rich in cholesterol and sphingomyelin and lacking carbohydrate moieties were also observed by Gallier et al. (2010) (black dots incorporated on the surface of the MFGs). The amount of these sphingomyelin and cholesterol domains seemed to increase with increasing fat content verifying their lipophilic behavior towards the MFGs (Gallier et al., 2010; Lopez et al., 2011).

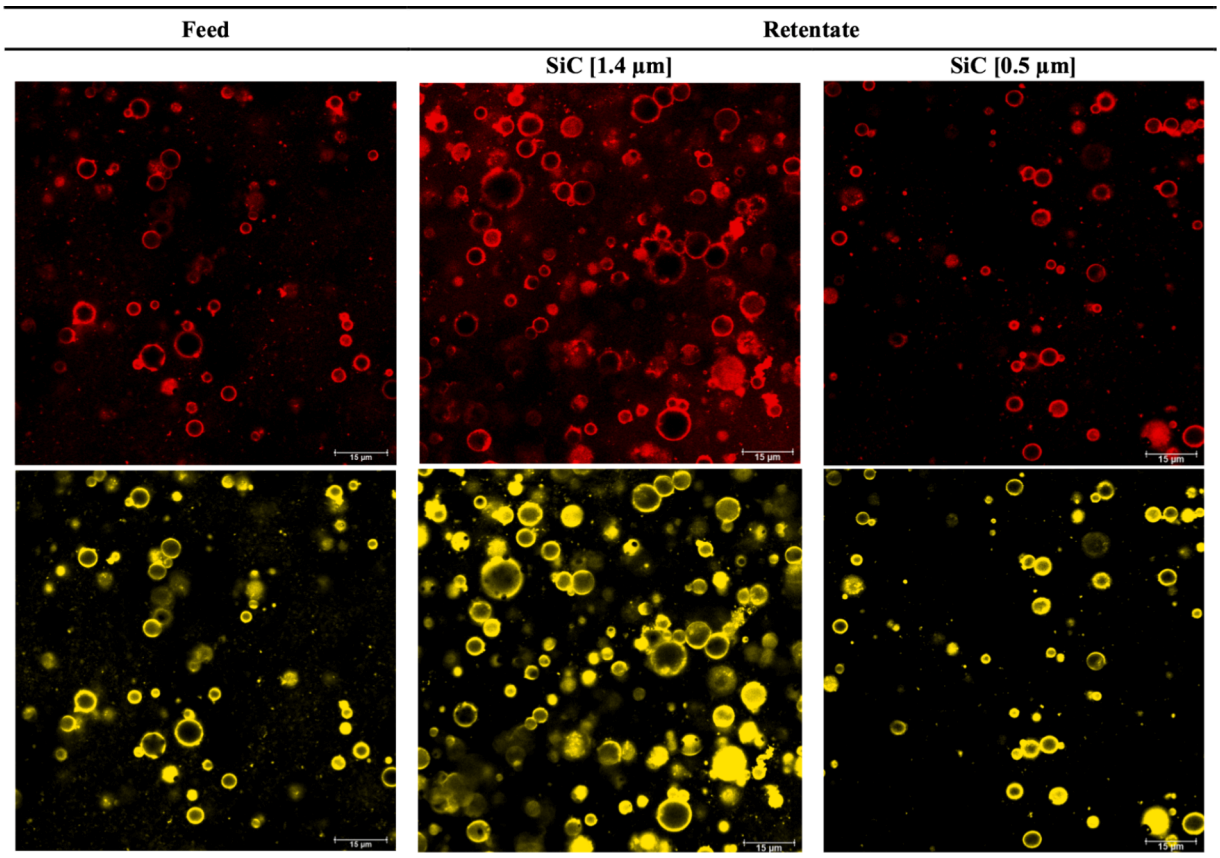

Fig. 5. Organization of glycoproteins and phospholipids in the membrane surrounding the milk fat globules of different size from the feed, the 1.4 µm VCR 4 and 0.5 µm VCR 3 membrane processing. Confocal Laser scanning microscopy images are shown corresponding to the emission fluorescence of Rhod-PE (**yellow**) labeling **phospholipids** and of the WGA-488 (**red**) used to label **glycoprotein**s. Scale bars are indicated on the figure of 15 µm.

Fig. 6 shows the permeate streams. The 1.4 µm permeate showed intact fat globules similar to the raw milk used as feed, but with a much lower MFG mean volume size and fat concentration (Table 1). The 1.4 µm permeate micrographs did not show any changes before or after the heating to 50 °C feeding it to the 0.5 µm membrane process.

The 0.5 µm permeate micrographs show different characteristics of the MFGs after processing. Small intact fat globules with limited interactions were observed. The tiny fat globules in this sample were though hard to conclude if they were too small to be well stained due to smearing of the staining, which might propose, that some of the MFGs are disrupted into smaller globules with altered shape. In addition, images of clustered globules were observed in the 0.5 µm permeate, with highly smeared areas, where the MFGs form aggregate-like structures. Clearly, interactions between the globules are formed either by protein–protein bindings on the surface of the MFGM or by the disruption of the MFGM causing MFGM sharing or protein adherence from nearby globules. The aggregates verifies the observations in the particle size distribution (Fig. 2 and Table 1) in the 0.5 µm permeate and the larger volume mean diameter.

The MFGM disruption is related to a locally induced pressure in the membrane pores. Larger MFGs (>0.5 µm) may enter the membrane pores due to increased flexibility at the processing temperature of 50 °C, here they are able to sterically obstruct the membrane pores during the filtration process. This leads to a gradual local pressure build-up on top of the globules nestled within the pores. The accumulating pressure will increase the molecular interactions between the permeating components as caseins, whey proteins and fat. Consequently, the increased pressure will induce shear forces, causing damage to the MFGs and disrupting the MFGM. The pore interactions and disruption of the MFGM of the involved MFGs will cause either the fat globules to coalesce into larger MFGs with a shared membrane though with milk proteins substituting for lack of membrane material. An alternative will be aggregate formation, where the small MFGs share membrane, sticking together at local spots with disrupted MFGM causing either protein–-protein interactions or fat-fat interactions by intermolecular forces.

3.3.2. *Milk fat globule integrity*

The structural and compositional changes at the surface of the MFGs may promote casein adherence to MFGs, and consequently changes the electrokinetic potential. The zeta potential for the generated samples for the feed and VCR 2–4 of the 1.4 and 0.5 µm membranes can be observed in Fig. 7A, whereas the zeta potential of the 1.4 and 0.5 µm permeate is shown in Fig. 7B. The initial raw milk used as feed showed a zeta potential of -27.00 ± 0.93 mV. The retentate streams of the 1.4 µm membrane showed a significant decrease from feed (-27.00 ± 0.93 mV) to VCR 4 (-35.23 ± 1.08 mV). The major changes in the retentates compared to the feed samples is explained by the milk protein adherence at the surface of the MFGM, where the 0.5 µm retentate had a low zeta potential of -32.40 ± 2.21 mV. Jukkola et al. (2019) proposed that the shear induced stress from pumping and the reduction of minerals in the retentate stream causes a release of MFGM components. Fig. 7B shows that there was a clear significant decrease in zeta potential for the two permeate samples. The difference is associated to the long pumping time and decreased pore size, which the MFGs in the 0.5 µm permeate, are exposed to (18 and 69 min, Fig. 1). The mechanism explaining the dissociation of MFGM components and substitution with milk proteins might be present in the interior pores. The pressure build-up in the obstructed pores might along with the increased shear forces form these protein-MFGM substitutions inside the pores or cause re-assembling in the final permeate.

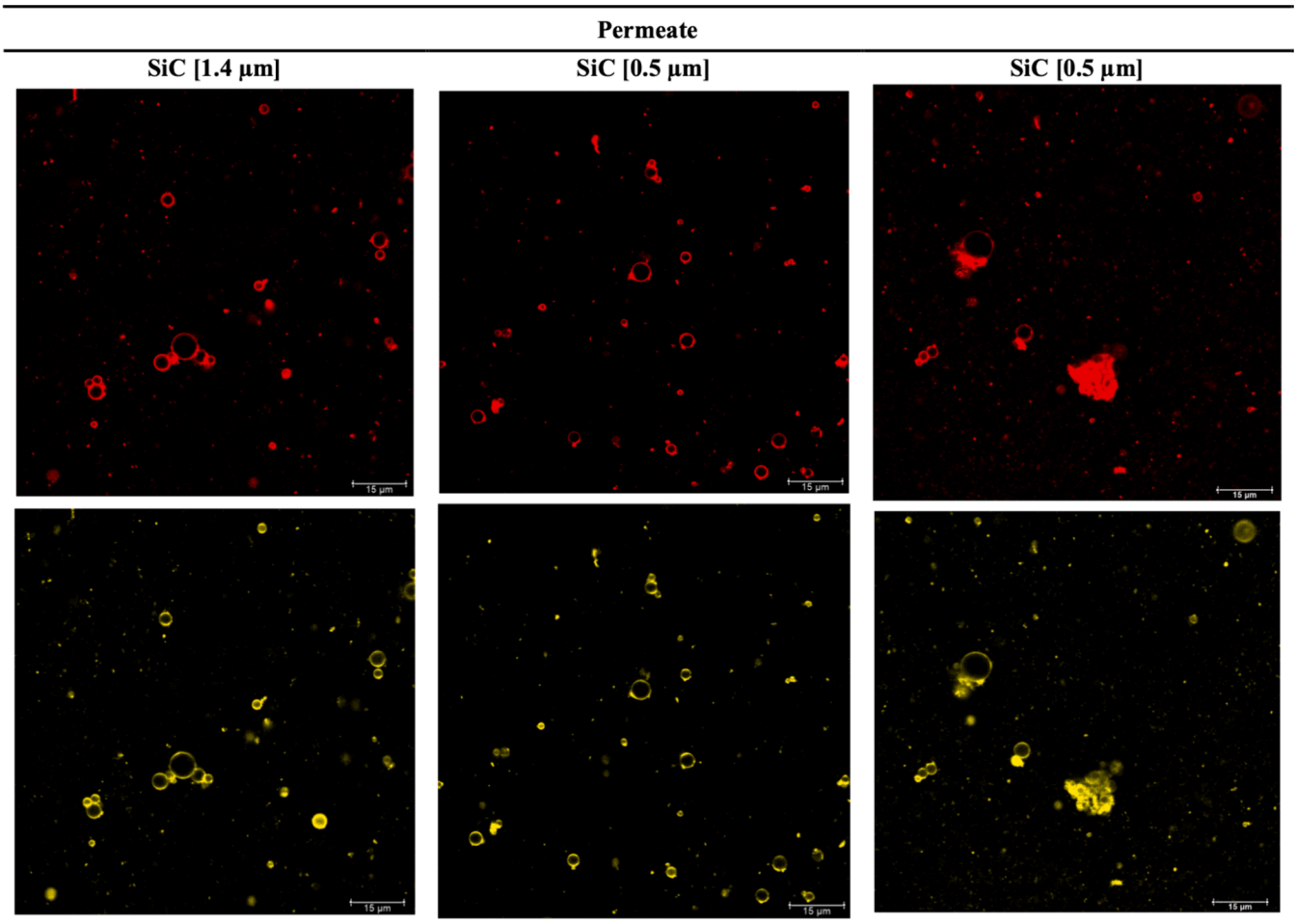

Fig. 6. Organization of glycoproteins and phospholipids in the membrane surrounding the milk fat globules of different size from the 1.4 µm and 0.5 µm permeate. In addition, images of larger aggregates found in the 0.5 µm are shown. Confocal Laser scanning microscopy images are shown corresponding to the emission fluorescence of Rhod-PE (**yellow**) labeling **phospholipids** and of the WGA-488 (**red**) used to label **glycoproteins**. Scale bars are indicated on the figure of 15 µm.

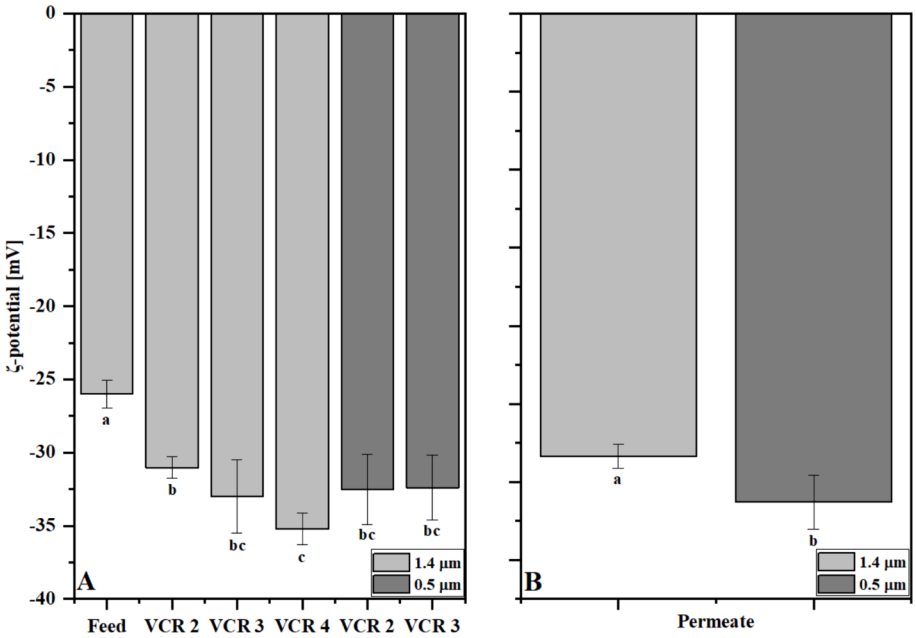

Fig. 7. Zeta-potential of A) feed and retentate streams (VCR 2–4) for the 1.4 and 0.5 µm membrane and B) Permeate stream for the 1.4 and 0.5 µm membrane. Values are presented as mean ± standard deviation; superscripts $^{a-c}$ ($P \leq 0.05$) denotes significant differences between samples.

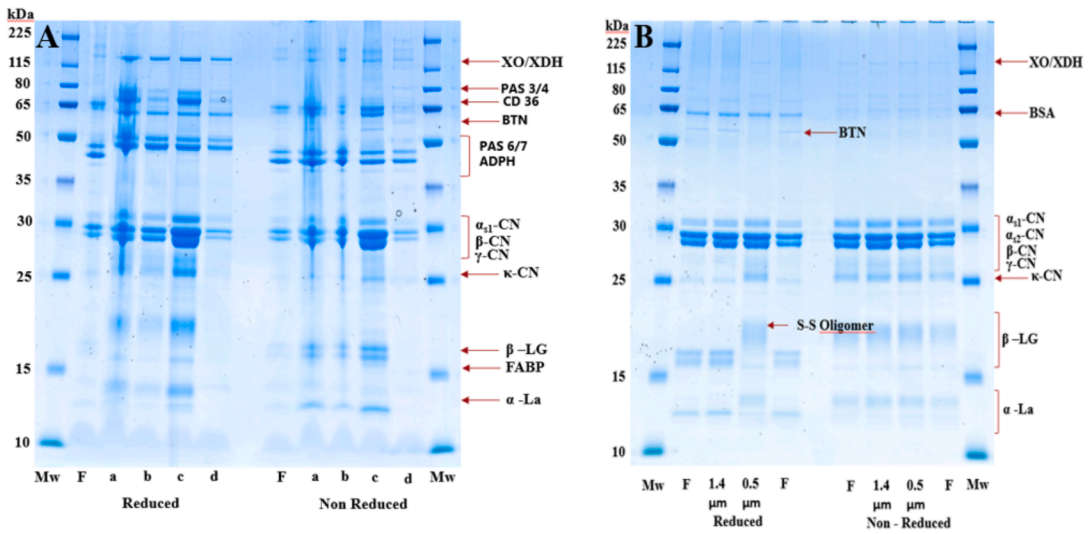

Fig. 8. Sodium dodecylsulphate-polyacrylamide gel electrophoresis of milk fat globule membrane related proteins in (A) Retentate and permeate samples where F. Feed, a. 1.4 μm permeate, b. 1.4 μm retentate VCR 4 c. 0.5 μm retentate VCR 3 and d. 0.5 μm permeate. (B) Milk proteins in permeate samples with F. Feed, 1.4 μm permeate and 0.5 μm of both reduced and non-reduced samples. Mw indicates the molecular mass marker. HMW. High Molecular weight, XO/XDH. Xanthine oxidase/Dehydrogenase, PAS. Periodic acid Schiff, CD36. Cluster of differentiation, BTN. Butyrophillin, ADPH. adipophillin, CN. Casein, LG. Lactoglobulin, La. Lactalbumin. All the proteins were identified by molecular mass and band length and compared with previous studies (Hansen et al., 2019; Mather, 2000; Xu et al., 2015; Yang et al., 2021; Ong et al., 2010).

To further study the proteins associated to the MFGs the retentates and permeates were analyzed after washing to recover MFGM proteins (Fig. 8A) and without washing for the permeates (Fig. 8B). The bands in Fig. 8A show the presence of MFGM proteins as xanthine oxidase, xanthine dehydrogenase (XO/XDH), Schiff base 3, 4, 6 and 7 (PAS 3/4 and PAS 6/7), cluster of differentiation 36 (CD36) and butyrophillin (BTN). Clearly these proteins are lost to the 1.4 μm permeate during the filtration, but PA 3/4 and CD 36 were concentrated by the 0.5 μm membrane, which though requires further investigation and quantification.

The bands from the 1.4 μm permeate containing small MFGs (D [4,3] = 1.82 ± 0.14 μm) showed the presence of both membrane related proteins, and caseins and whey proteins. A decreased amount of caseins and especially the whey proteins β-lactoglobulin (β-LG) and α-lactalbumin (α-La) were observed in the 1.4 μm retentate. A band with high intensity for caseins were also observed for the 1.4 μm retentate VCR 4. This band indicates that even limited processing to the MFGs will cause some casein adherence to the MFGM as previously observed by Hansen et al. (2020) and Jukkola et al. (2019).

Fig. 8B shows milk proteins present in the feed, the 1.4 μm permeate and 0.5 μm permeate. These gels (reduced) also show some of the MFGM related proteins as xanthine oxidase and butyrophillin due to their high molecular weight and their orientation towards the serum phase in the MFGM. The feed and 1.4 μm permeate showed very similar protein profiles for both reduced and non-reduced samples, with a clear band for bovine serum albumin, caseins and the whey proteins. Surprisingly, the 0.5 μm permeate showed a different behavior, with very limited intensity for butyrophillin and increased intensity for κ-casein in the reduced samples. The increased κ-casein intensity indicates that the caseins have undergone surface modifications consequently causing a higher content of κ-casein in the liquid phase compared to both the feed and the 1.4 μm permeate. The tailing band between 15 and 25 kDa for the 0.5 μm permeate might be directly associated to disulfide-linked protein oligomers, which are unable to undergo reduction by dithiothreitol (Yang et al., 2021). The large aggregates in Fig. 6 will sterically repulse the reduction by cluster formation of MFGs, caseins and whey proteins. Since the aggregate formation was not observed in the 1.4 μm permeate micrographs and the similar protein profile to the feed, may suggest, that the second heating step in the process did not form the aggregates. Though this heating step may have caused induced damage or interactions, which could lead to the potential aggregate formation.

4. Conclusion

The filtration performance and separation of fat from raw milk using SiC 1.4 μm and 0.5 μm membranes in series show the potential of effectively separate and concentrate fat from milk and produce unique streams in terms of fat and protein composition, casein:whey protein ratio and MFGM composition.

The 1.4 μm membrane separated the initial raw milk in 18 min with a 51 % flux decline resulting in retentate with 16.34 ± 0.37 % fat while the permeate had 0.5 ± 0.03 % fat. The 1.4 μm permeate was further separated using the 0.5 μm membrane in 69 min with 40 % flux decline achieving a retentate with 2.39 ± 0.56 % fat and produced a permeate with 0.19 ± 0.05 % fat, but resulted in a stream with casein:whey ratio of 50:50 compared to 80:20 in milk. The FA profiles indicated no significant differences between streams with different MFGs size, but the extended processing resulted in lipolysis of the long chain FAs resulting in an increase of short chain FAs in the fat rich retentates and the 0.5 μm permeate. Furthermore, both membranes showed high fat retention yields, 92.3 ± 1.5 % and 97.1 ± 0.2 % respectively for 1.4 μm and 0.5 μm membranes.

The membranes showed clear permeation of smaller MFGs in relation to the membrane pore size. Thus, fat rich retentates with MFGs ranging from D[4,3] = 4.1 to 4.4 μm were obtained using the 1.4 μm membrane while the 0.5 μm membrane produced retentates with smaller MFGs (D[4,3] ranging from 1.8 to 2.4 μm). The CLSM images showed intact MFGs while the SDS-PAGE gels showed differences in MFGMs proteins and concentration of Periodic Schiff base 3/4 and cluster of differentiation 36 that is worth further investigations.

Future studies on applications of these streams for commercial interest or health promoting effects would though have to be conducted.

Funding

The present study is a part of the platform for novel gentle processing supported by the Dairy Rationalisation Fund (DDRF), Arla Foods and University of Copenhagen.

CRediT authorship contribution statement

Tobias Dons: Writing – review & editing, Writing – original draft, Visualization, Validation, Methodology, Investigation, Formal analysis, Data curation, Conceptualization. **Jacob J.K. Kirkensgaard:** Writing – review & editing, Methodology, Investigation, Data curation. **Victor Candelario:** Writing – review & editing, Supervision. **Ulf Andersen:** Writing – review & editing, Supervision, Conceptualization. **Lilia Ahrné:** Writing – review & editing, Validation, Supervision, Project administration, Methodology, Investigation, Funding acquisition, Formal analysis, Conceptualization.

Declaration of competing interest

The authors declare that they have no known competing financial interests or personal relationships that could have appeared to influence the work reported in this paper.

Data availability

Data will be made available on request.

Acknowledgments

We thank the Centre for Advanced Bioimaging (CAB) University of Copenhagen, for the possibility to borrow their equipment for imaging. This study is part of the Platform for Novel Gentle Processing supported by the Dairy Rationalisation Fund (DDRF), Copenhagen University and Arla Foods.

References

Buldo, P., Kirkensgaard, J. J. K., & Wiking, L. (2013). Crystallization mechanisms in cream during ripening and initial butter churning. *Journal of Dairy Science, 96*(11), 6782–6791. https://doi.org/10.3168/jds.2012-6066

Buldo, P., Larsen, M. K., & Wiking, L. (2013). Multivariate data analysis for finding the relevant fatty acids contributing to the melting fractions of cream. *Journal of the Science of Food and Agriculture, 93*(7), 1620–1625. https://doi.org/10.1002/jsfa.5934

Chai, C., Oh, S., & Imm, J. Y. (2022). Roles of milk fat globule membrane on fat digestion and infant nutrition. *Food Science of Animal Resources, 42*(3), 351–371. https://doi.org/10.5851/kosfa.2022.e11

Chenchaiah, M., Muthukumarappan, K., & Metzger, L. E. (2013). Application of membrane separation technology for developing novel dairy food ingredients. *Journal of Food Processing & Technology, 04*(09). https://doi.org/10.4172/2157-7110.1000269

Deeth, H. C. (2006). Lipoprotein lipase and lipolysis in milk. *International Dairy Journal, 16*(6), 555–562. https://doi.org/10.1016/j.idairyj.2005.08.011

Deeth, H. C. (2011). Lipolysis and hydrolytic rancidity. In *Encyclopedia of dairy science* (2nd ed., pp. 721–726). Elsevier.

Dewettinck, K., Rombaut, R., Thienpont, N., Le, T. T., Messens, K., & Van Camp, J. (2008). Nutritional and technological aspects of milk fat globule membrane material. *International Dairy Journal, 18*(5), 436–457. https://doi.org/10.1016/j.idairyj.2007.10.014

Dickow, J. A., Larsen, L. B., Hammershøj, M., & Wiking, L. (2011). Cooling causes changes in the distribution of lipoprotein lipase and milk fat globule membrane proteins between the skim milk and cream phase. *Journal of Dairy Science, 94*(2), 646–656. https://doi.org/10.3168/jds.2010-3549

Dons, T., Candelario, V., Andersen, U., & Ahrné, L. (2024). Separation of milk fat using silicon carbide support ceramic membranes with different pore sizes. *Innovative Food Science & Emerging Technologies*. , Article 103671. https://doi.org/10.1016/j.ifset.2024.103671

Dons, T., Candelario, V., Andersen, U., & Ahrné, L. M. (2023). Gentle milk fat separation using silicon carbide ceramic membranes. *Innovative Food Science & Emerging Technologies, 84*, Article 103299. https://doi.org/10.1016/j.ifset.2023.103299

France, T. C., Kelly, A. L., Crowley, S. V., & O'mahony, J. A. (2021). Cold microfiltration as an enabler of sustainable dairy protein ingredient innovation. *Foods, 10*(9). https://doi.org/10.3390/foods10092091

Gallier, S., Gragson, D., Jiménez-Flores, R., & Everett, D. (2010). Using confocal laser scanning microscopy to probe the milk fat globule membrane and associated proteins. *Journal of Agricultural and Food Chemistry, 58*(7), 4250–4257. https://doi.org/10.1021/jf9032409

Hageman, J. H. J., Danielsen, M., Nieuwenhuizen, A. G., Feitsma, A. L., & Dalsgaard, T. K. (2019). Comparison of bovine milk fat and vegetable fat for infant formula: Implications for infant health. In *International Dairy Journal* (Vol. 92, pp. 37–49). Elsevier Ltd. doi: 10.1016/j.idairyj.2019.01.005.

Hansen, S. F., Petrat-Melin, B., Rasmussen, J. T., Larsen, L. B., Ostenfeld, M. S., & Wiking, L. (2018). Placing pasteurisation before or after microfiltration impacts the protein composition of milk fat globule membrane material. *International Dairy Journal, 81*, 35–41. https://doi.org/10.1016/j.idairyj.2017.12.015

Hansen, S. F., Wiking, L., Larsen, L. B., Rasmussen, J. T., Scientist, S., Hammershøj, M., Ahrné, L., & Lewis, M. J. (2019). *Milk fat globule membrane isolation with higher quality and stability*.

Holzmüller, W., Müller, M., Himbert, D., & Kulozik, U. (2016). Impact of cream washing on fat globules and milk fat globule membrane proteins. *International Dairy Journal, 59*, 52–61. https://doi.org/10.1016/j.idairyj.2016.03.003

Kaufmann, N., Kirkensgaard, J. J. K., Andersen, U., & Wiking, L. (2013). Shear and rapeseed oil addition affect the crystal polymorphic behavior of milk fat. *JAOCS, Journal of the American Oil Chemists' Society, 90*(6), 871–880. https://doi.org/10.1007/s11746-013-2226-z

Lopez, C., Briard-Bion, V., Ménard, O., Beaucher, E., Rousseau, F., Fauquant, J., Leconte, N., & Robert, B. (2011). Fat globules selected from whole milk according to their size: Different compositions and structure of the biomembrane, revealing sphingomyelin-rich domains. *Food Chemistry, 125*(2), 355–368. https://doi.org/10.1016/j.foodchem.2010.09.005

Lopez, C., Madec, M. N., & Jimenez-Flores, R. (2010). Lipid rafts in the bovine milk fat globule membrane revealed by the lateral segregation of phospholipids and heterogeneous distribution of glycoproteins. *Food Chemistry, 120*(1), 22–33. https://doi.org/10.1016/j.foodchem.2009.09.065

Mather, I. H. (2000). A review and proposed nomenclature for major proteins of the milk-fat globule membrane. In *Journal of Dairy Science* (Vol. 83, Issue 2, pp. 203–247). American Dairy Science Association. doi: 10.3168/jds.S0022-0302(00)74870-3.

McCarthy, N. A., Wijayanti, H. B., Crowley, S. V., O'Mahony, J. A., & Fenelon, M. A. (2017). Pilot-scale ceramic membrane filtration of skim milk for the production of a protein base ingredient for use in infant milk formula. *International Dairy Journal, 73*, 57–62. https://doi.org/10.1016/j.idairyj.2017.04.010

Michalski, M. C., Cariou, R., Michel, F., & Garnier, C. (2002). Native vs. damaged milk fat globules: Membrane properties affect the viscoelasticity of milk gels. *Journal of Dairy Science, 85*(10), 2451–2461. https://doi.org/10.3168/jds.S0022-0302(02)74327-0

Michalski, M. C., Leconte, N., Briard-Bion, V., Fauquant, J., Maubois, J. L., & Goudédranche, H. (2006). Microfiltration of raw whole milk to select fractions with different fat globule size distributions: Process optimization and analysis. *Journal of Dairy Science, 89*(10), 3778–3790. https://doi.org/10.3168/jds.S0022-0302(06)72419-5

Muthusamy, D. (2022). Milk fat globular membrane: Composition, structure, isolation, technological significance and health benefits. In *Dairy processing - From basics to advances [working title]*. IntechOpen. https://doi.org/10.5772/intechopen.106926.

Ong, L., Dagastine, R. R., Kentish, S. E., & Gras, S. L. (2010). The effect of milk processing on the microstructure of the milk fat globule and rennet induced gel observed using confocal laser scanning microscopy. *Journal of Food Science, 75*(3). https://doi.org/10.1111/j.1750-3841.2010.01517.x

Qi, T., Yang, D., Chen, X., Qiu, M., & Fan, Y. (2022). Rapid removal of lactose for low-lactose milk by ceramic membranes. *Separation and Purification Technology, 289*. https://doi.org/10.1016/j.seppur.2022.120601

Reig, M., Vecino, X., & Cortina, J. L. (2021). Use of membrane technologies in dairy industry: An overview. *Foods, 10*(11). https://doi.org/10.3390/foods10112768

Thum, C., Roy, N. C., Everett, D. W., & McNabb, W. C. (2023). Variation in milk fat globule size and composition: A source of bioactives for human health. In *Critical reviews in food science and nutrition* (Vol. 63, Issue 1, pp. 87–113). Taylor and Francis Ltd. doi: 10.1080/10408398.2021.1944049.

Truong, T., Lopez, C., Bhandari, B., & Prakash, S. (2020). Dairy fat products and functionality. In *Dairy fat products and functionality*. Springer International Publishing. https://doi.org/10.1007/978-3-030-41661-4.

Wiking, L., Gregersen, S. B., Hansen, S. F., & Hammershøj, M. (2022). Heat-induced changes in milk fat and milk fat globules and its derived effects on acid dairy gelation – A review. In *International Dairy Journal* (Vol. 127). Elsevier Ltd. doi: 10.1016/j.idairyj.2021.105213.

Xu, S., Walkling-Ribeiro, M., Griffiths, M. W., & Corredig, M. (2015). Pulsed electric field processing preserves the antiproliferative activity of the milk fat globule membrane on colon carcinoma cells. *Journal of Dairy Science, 98*(5), 2867–2874. https://doi.org/10.3168/jds.2014-8839

Yang, S., Suwal, S., Andersen, U., Otte, J., & Ahrné, L. (2021). Effects of pulsed electric field on fat globule structure, lipase activity, and fatty acid composition in raw milk and milk with different fat globule sizes. *Innovative Food Science and Emerging Technologies, 67*. https://doi.org/10.1016/j.ifset.2020.102548